Title

DISLOCATION DAMPING IN ALUMINUM AT HIGH STRAIN-RATES

Permalink

https://escholarship.org/uc/item/3tq9z8jd

Authors

Ferguson, W.G.
Kumar, A.
Dorn, J.E.

Publication Date

1966-09-01

UCRL-17106

University of California

Ernest O. Lawrence Radiation Laboratory

DISLOCATION DAMPING IN ALUMINUM AT HIGH STRAIN-RATES

Submitted to Journal of Applied Physics

UCRL-17106

UNIVERSITY OF CALIFORNIA
Lawrence Radiation Laboratory
Berkeley, California

AEC Contract No. W-7408-eng-48

DISLOCATION DAMPING IN ALUMINUM AT HIGH STRAIN-RATES

W. G. Ferguson, A. Kumar and J. E. Dorn

September, 1966

DISLOCATION DAMPING IN ALUMINUM AT HIGH STRAIN RATES

W. G. Ferguson, A. Kumar and J. E. Dorn

Inorganic Materials Research Division, Lawrence Radiation Laboratory,
and Department of Mineral Technology, College of Engineering,
University of California, Berkeley, California

August, 1966

ABSTRACT

Impact shear tests of the Kolsky Thin Wafer type were used to determine the effect of temperature and strain-rate on the critical resolved shear stress for slip in aluminum single crystals at strain-rates of 10^4 sec^{-1} and in the temperature range 20°K to 500°K. The aluminum deformed in a viscous manner in that the flow stress was proportional to the plastic strain-rate. The behavior was found to be temperature dependent. The results were discussed in terms of dislocation damping models where the friction force acting on a dislocation results from, at cryogenic temperatures, electronic viscosity, and at higher temperatures, phonon viscosity. The theories predicted general agreement as to the magnitude of the observed damping but some discrepancy was found to exist between the observed and theoretical temperature dependence of the damping.

I. INTRODUCTION

Previous investigations[1,2,3] into the dynamic properties of materials have shown that over a wide range of strain-rates the effect of testing temperature on the plastic flow stress can be explained by the mechanism of thermal activation of dislocations over short range barriers. These thermally activated mechanisms of deformation can be visualized as follows. Under an applied shear stress the mobile dislocations move rapidly until various segments are arrested at barriers and the dislocations are momentarily held up. Under the random action of thermal vibrations, large enough thermal vibrations will occur which help the dislocations to overcome the barriers and move on. At a given shear stress, a higher testing temperature will decrease the average arrest periods of the dislocations at barriers because of the larger amplitude of thermal vibration and the strain-rate will increase. Similarly at constant temperature an increase in shear stress supplies a greater amount of strain energy to the dislocation and a correspondingly smaller thermal vibration can activate the process.

Figure 1 shows this type of behavior for aluminum single crystals tested in tension where the Schmid angles for $\{\bar{1}11\}$ <110> type slip are $90 - \chi_o \approx \lambda_o = 45° \pm 1°$.[4] τ_A is the athermal component of the applied stress and is due to long range barriers that cannot be penetrated by the dislocations by means of thermal activation. τ_T is due to short range barriers and can be overcome by the combination of applied stress $(\tau^* + \tau_A)$ plus thermal activation. When the applied stress is high enough to exceed $\tau_A + \tau_T$, the dislocations can be pushed past barriers without assistance from thermal fluctuations. To obtain stresses in excess of $\tau_A + \tau_T$ high strain-rates are necessary.

In some earlier work on polycrystalline aluminum, Hauser, Simmons and Dorn[1] obtained some data in the high stress, high strain-rate region using the Kolsky Thin Wafer technique.[5] It was found that because the material was rather strong and the maximum stress was limited by the testing machine, little data could be obtained in the high stress high strain-rate region. In subsequent work by Mukherjee, Ferguson, Barmore and Dorn[3] single crystals of β-AgMg were tested in shear impact. Although the shear type specimens permitted higher strain rates because of their smaller effective gauge length, the high strength of the β-AgMg crystals again limited the available data. Nevertheless, in both prior investigations a linear dependence of flow stress on strain-rate was found near the highest possible applied stresses. Recently Ferguson, Hauser and Dorn[6] examined the behavior of zinc single crystals deformed in basal shear at shear stresses higher than the thermally activated stress range and found that the applied shear stress was proportional to the shear strain-rate. The behavior was independent of temperature for the temperature range investigated, 300°K to 653°K.

In the high strain-rate, high stress region various dissipative mechanisms prescribe the dislocation motion. Mason,[7,8,9] Lothe[10] and Dorn, Mitchell and Hauser[11] have reviewed the various mechanisms proposed thus far and in all cases the theories predict that the friction stress on a dislocation should vary linearly with its velocity, thus making it difficult to distinguish between the theories. Even so the work on zinc by Ferguson, Hauser and Dorn[6] could be rationalized in terms of Mason's[12] dislocation damping model where the friction force acting on a dislocation results from phonon viscosity.

It was the object of the present investigation to critically examine the high stress, high strain-rate behavior at both high and low temperatures. For this purpose aluminum single crystals were chosen because their low strength permitted high strain-rates to be obtained and their ductility allowed testing at cryogenic temperatures.

II. EXPERIMENTAL TECHNIQUES

The Kolsky Thin Wafer technique was used as the method for obtaining high stresses and high strain-rates and the specimens were tested in shear because this enabled a small gauge length to be used, which enhanced the upper strain rate limit. A description of the dynamic impact machine employed during the present investigation has been reported previously by Hauser[13] and the method of analyzing the results obtained for this type of loading has also been described.[13] The configuration of the loading bars used to obtain dynamic shear is shown in Fig. 2b.

The specimens were prepared for testing as follows.

(1) A sphere 1 in. in diameter was grown in a carbon mold from high purity (99.995 wt. pct.) aluminum under an argon atmosphere using a modified Bridgman technique.

(2) The sphere was then used as a seed to grow an oriented single crystal bar with a cross section of 1/4 in. by 1/8 in. with the {111} plane perpendicular to the axis of the bar and the slip direction parallel

to its 1/4 in. side. The orientation of the crystal bars was checked by the Laue, back reflection x-ray technique and only those found to be within ±1 deg. of the required orientation were used.

(3) Specimens 3/8 in. long were cut from the bar and double gauge sections, 0.050 in. long were spark machined in them as shown in Fig. 2a. The spark machined specimens were given a light chemical etch in a solution of 9 parts HCl, 3 parts HNO_3, 2 parts HF and 5 parts H_2O to insure all surface deformation from spark cutting was removed.

The tests at 500°K were conducted using a small Kanthal wound resistance furnace to enclose the specimen and those at 77°K by immersing the specimen in a bath of liquid nitrogen. At 20°K the specimen was contained in a small cylindrical cavity in a large block of styrofoam. The impact bars were inserted in each end of the cavity and the specimen was cooled by a constant stream of liquid helium which was allowed to vent to the atmosphere through a small hole in the styrofoam container. The temperature was measured using a copper-constantan thermocouple that had previously been calibrated at 4.2°K, 77°K and 273°K. Interpolated readings of the temperatures between 4.2°K and 77°K were made using the tables of Powell, Bunch and Corruccini.[14] The temperature could be determined to within ±4°K at 20°K.

The resistivity of an aluminum single crystal rod was determined at 4.2°K, 77°K and 273°K by immersing the rod incryostats containing the appropriate coolant and measuring the voltage drop with a nano-voltmeter.

III. RESULTS AND DISCUSSION

The experimental data obtained are plotted in Fig. 3 as shear stress τ at initial plastic flow versus plastic, shear strain-rate $\dot{\gamma}$. It can be seen from Fig. 3, that within the experimental scatter the shear stress is proportional to the shear strain-rate and the behavior is temperature dependent. The straight lines drawn through the experimental points can be described by the following type equation,

$$\tau - \tau_B = \alpha\dot{\gamma} \qquad (1)$$

where τ_B = the back stress as defined in Fig. 3 and α = the slope of the lines. α was determined using a back stress of 300 p.s.i. and is plotted in Fig. 4 as a function of temperature. It can be seen from Fig. 4 that α is temperature dependent and increases by 1.55 times between 500°K and 20°K. Ferguson, Hauser and Dorn[6] did not detect any temperature dependence of α for zinc single crystals in the temperature range they investigated, 300°K to 653°K. The magnitude of α for zinc was 5×10^3 dyne-sec/cm^2 whereas in the present investigation α at 500°K is 1×10^4 dyne-sec/cm^2 showing a two fold increase over the value for zinc.

The data in Fig. 3 clearly show that the material is deforming in a viscous manner and hence, the dislocation motion must be damped by some energy absorbing mechanism. Damping of the above type has been observed by a number of investigators[7,8,15] doing internal friction studies. These investigators use the Granato-Lücke[16] theory to evaluate internal friction data and obtain a damping constant B defined as follows;

$$F = BV = \tau b \qquad (2)$$

where F = the force on the dislocation, V = the dislocation velocity, b = Burger's vector and B = the damping constant. B can be related to the α in Eq. (1) using the relationship $\dot{\gamma} = \rho b V$, where ρ is the mobile dislocation density. Then

$$B = \rho b^2 \alpha \qquad (3)$$

where the mobile dislocation density is the only unknown. Taking b for aluminum as 2.86×10^{-8} cm, α from the data at 300°K as 1.23×10^4 dyne-sec/cm^2 and assuming $\rho = 2 \times 10^8$ cm^{-2}, then B at 300°K = 2.01×10^{-3} dyne-sec/cm^2. For comparison, experimental values of B determined by internal friction measurements and dislocation velocity measurements, using etch-pit techniques, are shown in Table 1.

Using a dislocation density of 2×10^8 cm^{-2} and assuming that it is not appreciably affected by temperature (it should in fact decrease slightly with increasing temperature) the damping constant B was determined from α and plotted in Fig. 5. Also shown in Fig. 5 is the mean of the damping constants obtained by Sylwestrowicz[23] for aluminum single crystals, damping constants determined from the attenuation data of Hutchison and Rogers[24] on polycrystalline aluminum and damping constants for copper as determined by Alers and Thompson.[20] Because of the limited information available, the damping constants determined from the low frequency, attenuation data of Hutchison and Rogers[24] were calculated by making the B at 297°K the same as that obtained by Sylwestrowicz[23] and using the fact that the Granato-Lücke[16] theory predicts that at low frequencies the amplitude-independent attenuation is proportional to B at constant frequency. Although this method does not give the absolute values of the damping constants for the data of Hutchison and Rogers,[24] it does show the temperature dependence of their data. It can be seen from Fig. 5 that there is a discrepancy between the temperature dependence of the damping constants obtained by the internal friction methods and the method employed in the present investigation.

In the high stress region the dislocations are traversing the crystal with little hindrance from lattice imperfections and the dislocation velocity is primarily limited by interactions with electrical and thermal waves. For thermal waves, at least three mechanisms have been proposed describing the interaction of phonons with dislocations. The first of these, due to Eshelby,[25] considers the energy loss associated with the thermoelastic effect as the dislocation moves through the crystal. Since screw dislocations produce only shear stresses in the crystal, the thermoelastic effect which is due to the difference of effective temperature in an extended and compressed lattice does not produce a drag for these dislocations. Even for edge dislocations this source of damping is much smaller than the other two that will be considered.[9]

The second source of dislocation damping considered is the scattering of thermal phonons by moving dislocations, first derived by Leibfried.[26] The damping constant B for this source of damping takes the form

$$B = \frac{aE_o}{10V_s} \tag{4}$$

where a = lattice parameter, E_o = thermal energy density and V_s = shear wave velocity. Taking a for aluminum as 4.05×10^{-8} cm, V_s = $= 3.03 \times 10^5$ cm/sec and determining E_o from tables[27] using $\theta_D = 396°K$, the magnitude of B for phonon scattering in aluminum can be obtained. The results are tabulated in Table 2 and plotted in Fig. 6.

The third source of damping is related to phonon viscosity. This mechanism, first derived by Mason,[9,12] regards the lattice vibrations as a viscous phonon gas. When a dislocation moves through this gas, the gas is stirred up, energy is dissipated and a frictional stress on the dislocation results. The damping constant B for this source of damping takes the form

$$B = \frac{b^2\eta}{8\pi a_o^2} \text{ for screw dislocations} \qquad (5)$$

where b = Burger's vector, a_o = effective core radius of the dislocation and η = viscosity of the phonon gas. Taking b for aluminum as 2.86×10^{-8} cm and using a value of $\frac{3}{4}$ b for a_o as was done by Suzuki, Ikushima and Aoki[15] and Mason,[12] who give justification for doing this, Eq. (5) reduces to

$$B = 0.071\ \eta \qquad (6)$$

η can be shown from gas kinetic theory to be

$$\eta = \frac{D.E_o.K_p}{\rho C_v.\bar{V}^2} \qquad (7)$$

where E_o = thermal energy density, K_p = lattice thermal conductivity,

$\bar{V}$ = Debye average velocity, ρC_v = specific heat per unit volume and D = a nonlinear constant.

It is necessary to separate the lattice thermal conductivity K_p from the total thermal conductivity K_T which is largely determined by electron motion. This can be done for materials for which the thermal conductivity is measured as a function of impurity content but this has not been done for aluminum. Leibfried and Schlömann[28] have calculated the lattice thermal conductivity, using a simple model, for cubic crystals but the simple formulation of their result is only true for $T \geq \theta_D$ and does not give the correct temperature dependence for $T < \theta_D/10$. For this reason the lattice thermal conductivity was determined using the simple method outlined by Kittel[29] because although it gives only an approximate result it predicts the correct temperature dependence of K_p. The ratio of the thermal conductivity due to electrons K_e to that due to phonons K_p can be written as[29]

$$\frac{K_e}{K_p} = \frac{\rho C_e \, \bar{U}_e^{\,2} \, \tau_{ep}}{\rho C_v \, \bar{V}^2 \, \tau_{pe}} \tag{8}$$

where C_e = the electronic specific heat = 1.46×10^3 T ergs/cm^3 - °K, $\bar{U}_e$ = the Fermi velocity of the electrons = 1.43×10^8 cm/sec, $\bar{V}$ = the Debye average velocity = 3.7×10^5 cm/sec as determined by Anderson[30] and $\frac{\tau_{ep}}{\tau_{pe}}$ = the ratio of the electron-phonon relaxation time to the phonon-electron relaxation time which for metals of good purity is about $= 10^{-2}$.[29] K_p has been calculated and tabulated in Table 3 using the thermal conductivity data of Hall, Roder and Powell[31] and ρC_v determined from tables.[27] Using the above data η/D has been calculated from Eq. (7) and is also tabulated in Table 3.

The nonlinear constant D can be calculated from the third order elastic moduli[7] or evaluated by measuring the attenuation along directions in crystals for which the dislocations are not activated by the applied stress.[7] This latter method has been used by Mason[7] to calculate D for the shear mode of propagation in a number of crystals (see Table 4) and the former method has also been used[7] to determine D for both the longitudinal and shear modes of propagation in germanium, silicon and quartz. Recently Hiki and Granato[32] have measured the third order elastic moduli for copper, silver and gold and Mason[8] has calculated the D for the longitudinal mode of propagation in copper to be 42.6. As the third order elastic moduli of aluminum have not been measured and no attenuation data is available for which dislocations are not activated, the nonlinear constant D for this material cannot be evaluated directly. For the evaluation of B for phonon viscosity, D for the shear mode of propagation was taken as 15 which is not unreasonable when compared to the values obtained experimentally for copper and cadmium (see Table 4). The damping constant B for the phonon viscosity model is tabulated in Table 3 and plotted in Fig. 6.

For electrical waves a mechanism has been proposed by Mason[33,34] describing the interaction of electrons with dislocations. This mechanism is similar in principle to the phonon viscosity concept and the damping constant B takes the same form as Eq. (5). Taking $a_o = 10^{-7}$ cm, which is considered to be a reasonable value,[34] the value of the damping constant B for electronic viscosity becomes

$$B = 3.25 \times 10^{-3}\ \eta \qquad (9)$$

where η is the electronic viscosity. The electronic viscosity η can be determined in a manner analogous to the phonon viscosity by using the variables appropriate for an electron gas. The electronic viscosity then takes the form

$$\eta = \frac{9 \times 10^{11}\ \hbar^2\ (3\pi^2 N)^{2/3}}{5\ e^2 \rho_e} \qquad (10)$$

where $\hbar$ = Plank's constant divided by 2π, N = number of electrons per cc and ρ_e = the electrical resistivity in ohm centimeters. Taking $N = 6.06 \times 10^{22}\ \mathrm{cm}^{-3}$, $\hbar = 1.054 \times 10^{-27}$ erg sec and $e = 4.8 \times 10^{-10}$ e.s.u. then B for the electronic viscosity becomes

$$B = \frac{4.18 \times 10^{-11}}{\rho_e} \qquad (11)$$

Using the values of the electrical resistivity determined at 4.2°K, 77°K and 273°K and interpolating between these values using the data of Hall, Roder and Powell,[31] B for electronic viscosity was calculated, tabulated in Table 5 and plotted on Fig. 6.

It can be seen from Fig. 6 that for aluminum the phonon viscosity model predicts a damping constant B which is greater than that predicted by the phonon scattering model and that the sum of the phonon and electron viscosities shows a dip at about 80°K. Although no direct value for B was obtained in the present investigation because of the difficulty of measuring the mobile dislocation density it can be seen that for the assumed dislocation density of 2×10^8 cm^{-2} the electronic viscosity model shows reasonable agreement with the present results at very low temperatures. Similarly the phonon viscosity model shows reasonable agreement at high temperatures but, like the electronic viscosity model, fails to predict the observed temperature dependence of the experimental data obtained in the present investigation. Although the phonon and electron viscosity models fail to predict the temperature dependence of the present data they show reasonable agreement with the temperature dependence of the internal friction results of Hutchison and Rogers.[24] It is possible that the above theories may have to be modified before they can be applied to the analysis of the present data, because with internal friction measurements the dislocations are pinned at each end and only sweep out a small area when they vibrate, but in the present investigation, the dislocations sweep out very large areas as they move through the crystal, and in doing so come into contact with other dislocations and impurity atoms which probably modify the damping behavior.

IV. CONCLUSIONS

(1) If aluminum single crystals are deformed at a shear stress higher than the thermally activated stress range they behave in a viscous manner, in that the stress is proportional to the shear strain-rate.

(2) At stresses higher than the thermally activated stress range,

the stress strain-rate behavior is temperature dependent for the temperature range investigated, 20°K to 500°K.

(3) Mason's phonon and electron viscosity models for dislocation damping predict general agreement with the magnitude of the experimental results but some discrepancy exists between the observed and the theoretical temperature dependence of the damping behavior.

(4) If a mobile dislocation density of 2×10^8 cm^{-2} is assumed the present results yield damping constants B which range in magnitude from 1.71×10^{-3} $dynes\text{-}sec/cm^2$ at 500°K to 2.66×10^{-3} $dyne\text{-}sec/cm^2$ at 20°K.

ACKNOWLEDGMENTS

This research was conducted as part of the activities of the Inorganic Materials Research Division of the Lawrence Radiation Laboratory of the University of California. The authors wish to express their appreciation to the United States Atomic Energy Commission for its support of this work.

REFERENCES

1. F. E. Hauser, J. A. Simmons and J. E. Dorn, Response of Metals to High Velocity Deformation, V: F. Zackay, Ed., (Interscience, New York, 1961), 93.
2. T. L. Larsen, S. L. Rajnak, F. E. Hauser and J. E. Dorn, J. Mech. Phys. Solids, 12, 361 (1964).
3. A. K. Mukherjee, W. G. Ferguson, W. L. Barmore and J. E. Dorn, To be published, J. Appl. Phys. (Sept., 1966).
4. A. K. Mukherjee, J. D. Mote and J. E. Dorn, Trans. AIME, 233, 1559 (1965).
5. H. Kolsky, Proc. Roy. Soc. London, 62, 667 (1949).
6. W. G. Ferguson, F. E. Hauser, and J. E. Dorn, Submitted to Acta Met., 1966.
7. W. P. Mason, Physical Acoustics (Academic Press, 1966) Chap. II, VIII, 237.
8. W. P. Mason, Technical Report No. 28, Dept. Civil Eng., and Eng., Mech, Columbia University, New York (1966).
9. W. P. Mason, J. Accoustical Soc. of Am., 32, 458 (1960).
10. J. Lothe, J. Appl. Phys., 33, 2116 (1962).
11. J. E. Dorn, J. B. Mitchell and F. E. Hauser, Exp. Mech., 5, 353 (1965).
12. W. P. Mason, J. App. Phys., 35, 2779 (1964).
13. F. E. Hauser, Exp. Mech., 6, 395 (1966).
14. R. L. Powell, M. D. Bunch and R. J. Corruccini, Cryogenics, 1, 139 (1961).

15. T. Suzuki, A. Ikushima and M. Aoki, Acta Met., 12, 1231 (1964).
16. A. Granato and K. Lücke, J. Appl. Phys., 27, 583 (1956).
17. W. G. Johnston and J. J. Gilman, J. Appl. Phys., 30, 129 (1959).
18. E. Yu. Gutmanas, E. M. Nadgornyi and A. V. Stepanov, Soviet Physics Solid State, 5, 743 (1963).
19. A. Granato, A. Hikata and K. Lücke, Acta Met., 6, 470 (1958).
20. G. A. Alers and D. O. Thompson, J. Appl. Phys., 32, 283 (1961).
21. R. M. Stern and A. Granato, Acta Met., 10, 358 (1962).
22. O. M. Mracek Mitchell, J. Appl. Phys., 36, 2083 (1965).
23. W. D. Sylwestrowicz, J. Appl. Phys., 37, 535 (1966).
24. T. S. Hutchison and D. H. Rogers, J. Appl. Phys., 33, 792 (1962).
25. J. D. Eshelby, Proc. Roy. Soc. London, A197, 396 (1949).
26. G. Leibfried, Z. Physik, 127, 344 (1950).
27. American Institute of Physics Handbook, (McGraw-Hill Book Co., Inc., New York, 1963).
28. G. Leibfried and E. Schlömann, Nachr. Akad. Wiss. Gott., 11a, 71 (1954).
29. C. Kittel, Introduction to Solid State Physics, (John Wiley and Sons, New York, 1956), Second Edition.
30. O. L. Anderson, Physical Acoustics, Edited by W. P. Mason, (Academic Press, 1966), Chap. II, VIII, B.
31. W. J. Hall, H. M. Roder and R. L. Rowell, Proc. Fifth Int. Conf. on Low Temp. Physics and Chemistry, Edited by J. R. Dillinger (The University of Wisconsin Press, 1958).

32. Yosio Hiki and A. V. Granato, Phys. Review, 144, 411 (1966).

33. W. P. Mason, Appl. Phys. Letters, 6, 111(1965).

34. W. P. Mason, Phys. Review, 143, 229 (1966).

Table 1. Damping constant B at room temperature.

Material	LiF	NaCl	KCl	Quartz	Cu	Cu-0.13% Mn	Al
Dislocation Velocity Measurements	$7x10^{-4}$[17]	$2x10^{-4}$[18]					
Internal Friction Measurements	$1.3x10^{-3}$[15] $3.4x10^{-4}$[22]	$2x10^{-3}$[19]	$3.5x10^{-4}$[15]	$6x10^{-4}$[9]	$7.9x10^{-5}$[15] $6.0x10^{-5}$[9] $8.0x10^{-4}$[20] $6.5x10^{-4}$[21]	$4.5x10^{-4}$[15]	$2x10^{-3}$[23]

Table 2. Calculated values of B for phonon scattering as a function of temperature.

Temperature °K	25	50	75	100	200	300	400	500	600	700
E_o x 10^{-8} erg/cm^3	0.031	0.473	1.554	4.580	22.20	44.25	67.6	91.75	115.8	141.4
B x 10^5 dyne-sec/cm^2	0.004	0.06	0.2	0.6	3.0	5.9	9.0	12.3	15.5	18.9

Table 3. Calculated values of B for phonon viscosity as a function of temperature.

Temperature °K	25	40	50	70	100	200	300	400	500	700
$\rho C_v \times 10^{-7}$ erg/cm^3-°K	0.05	0.2	0.36	0.73	1.26	2.06	2.30	2.38	2.42	2.45
$E_o/\rho C_v$ °K	6.26	10.25	13.3	21.2	36.5	108	192.5	26[illegible]	379	[illegible]
$E_o/\rho C_v.\bar{V}^2 \times 10^{+10}$	0.47	0.76	0.96	1.59	2.76	8.55	15.7	24.2	33.6	55.5
$K_p \times 10^{-7}$ erg/sec-cm-°K	0.12	0.273	0.274	0.23	0.17	0.118	0.08	0.062	0.049	0.036
$\eta/D \times 10^3$ poise	0.056	0.208	0.263	0.368	0.525	1.00	1.26	1.49	1.65	2.02
$B \times 10^3$ dyne-sec/cm^2	0.06	0.22	0.28	0.39	0.56	1.07	1.35	1.59	1.75	2.14

Table 4. Non linear constant D

Material	Longitudinal D	Shear D	Remarks
Germanium	5.1	1.0	Measured[7]
Silicon	4.5	1.0	Measured[7]
Quartz	9.0	7.0	Measured[7]
LiF		4.0	Attenuation Measurements[7]
NaCl		2.07	Attenuation Measurements[7]
KCl		1.98	Attenuation Measurements[7]
KBr		2.24	Attenuation Measurements[7]
Zn	8		Attenuation Measurements[6]
Cd	75	31.4	Attenuation Measurements[8]
Cu	42.6		Measured[8,32]

Table 5. Calculated values of B for electronic-viscosity as a function of temperature.

Temperature °K	4	6	10	20	30	60	100	200	300	500	700
$\rho \times 10^8$ ohm-cm	1.47	1.47	1.47	2.0	3.2	0.133	0.42	0.017	0.03	0.055	0.08
$B \times 10^{+3}$ dyne-sec/cm^2	2.84	2.84	2.84	2.09	1.31	0.314	0.1	0.0246	0.014	0.0076	0.0052

FIGURE CAPTIONS

Figure 1. Effect of temperature and strain-rate on the flow stress of aluminum single crystals.[4]

Figure 2a. Specimen geometry.

Figure 2b. Shear bars used for dynamic testing.

Figure 3. Shear stress versus shear strain-rate for dynamic shear in aluminum single crystals.

Figure 4. The slope α of the shear stress-shear strain-rate curves versus temperature.

Figure 5. Experimental damping constants for aluminum and copper versus temperature.

Figure 6. Theoretical damping constants for phonon scattering, phonon viscosity and electronic viscosity in aluminum.

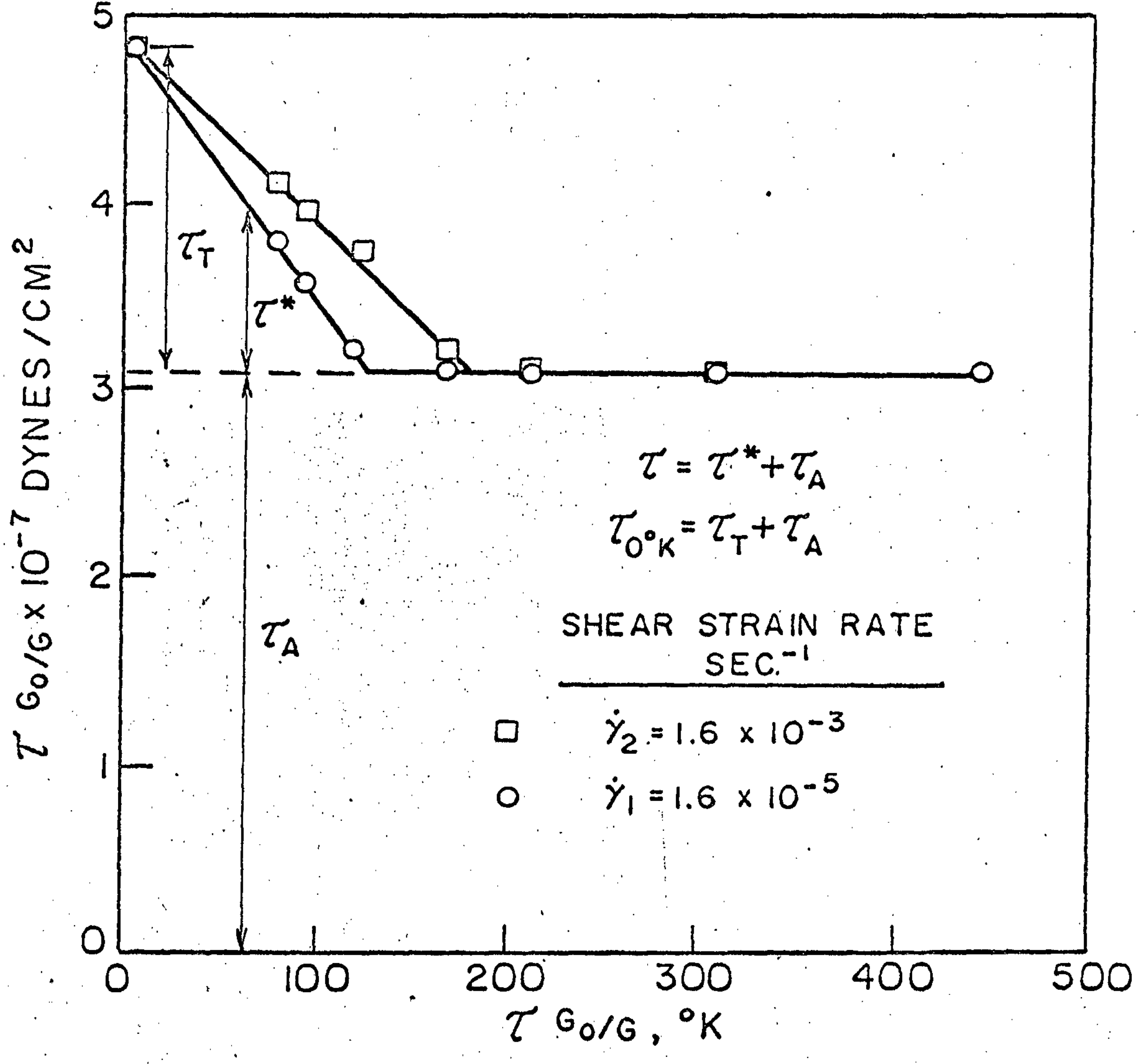

FIG. I EFFECT OF TEMPERATURE AND STRAIN RATE ON THE FLOW STRESS OF ALUMINUM SINGLE CRYSTALS.(4)

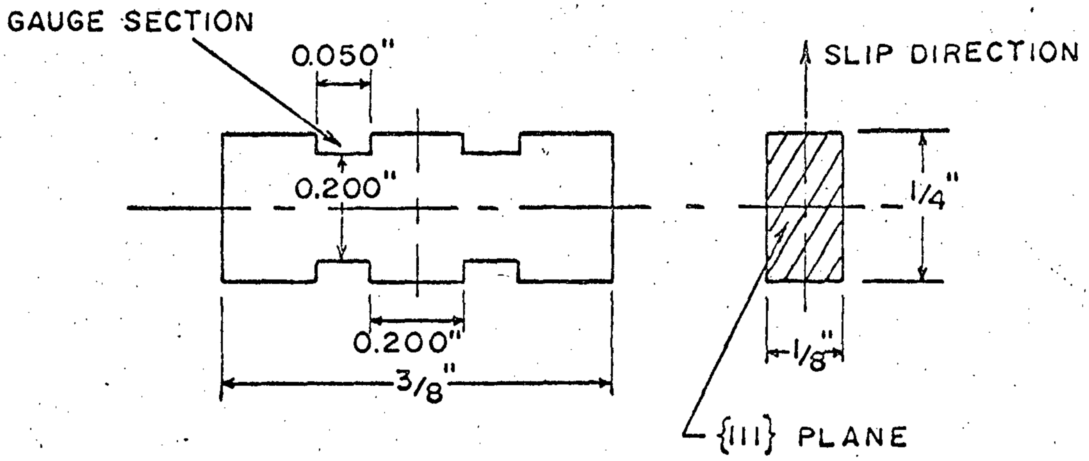

FIG. 2(a) SPECIMEN GEOMETRY.

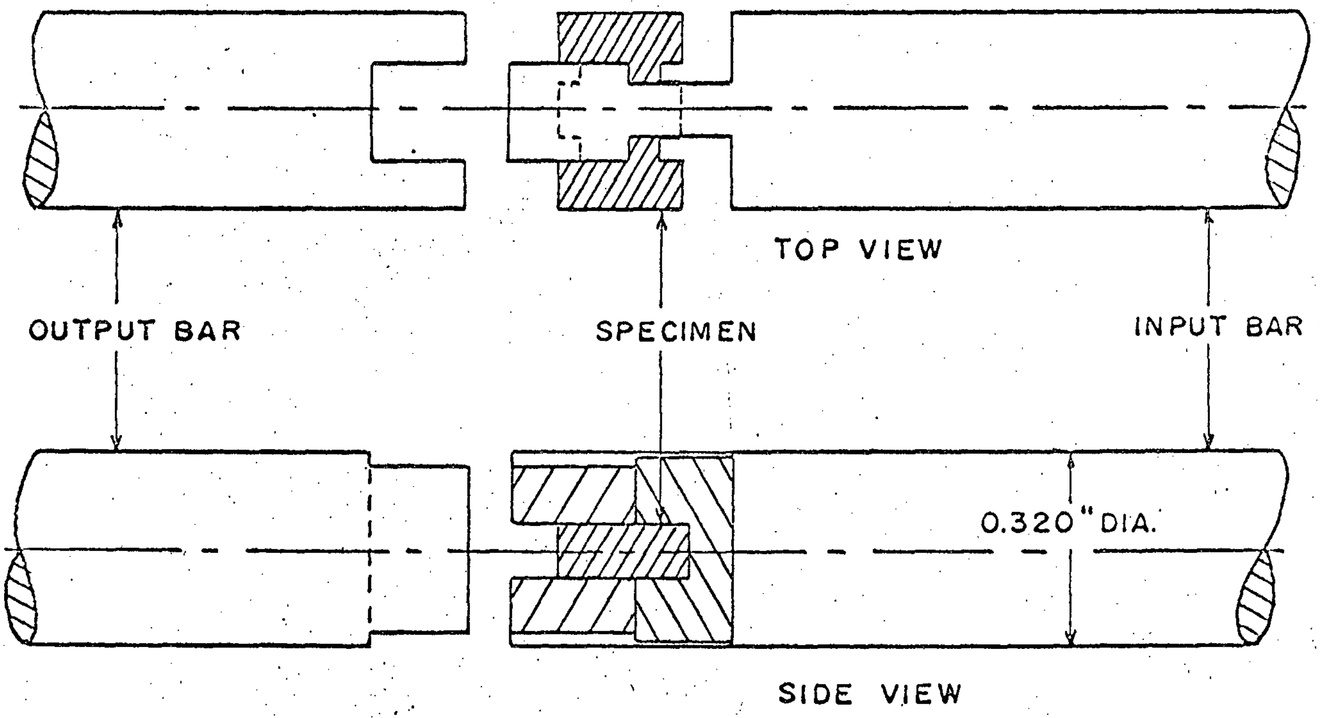

FIG. 2(b) SHEAR BARS USED FOR DYNAMIC TESTING.

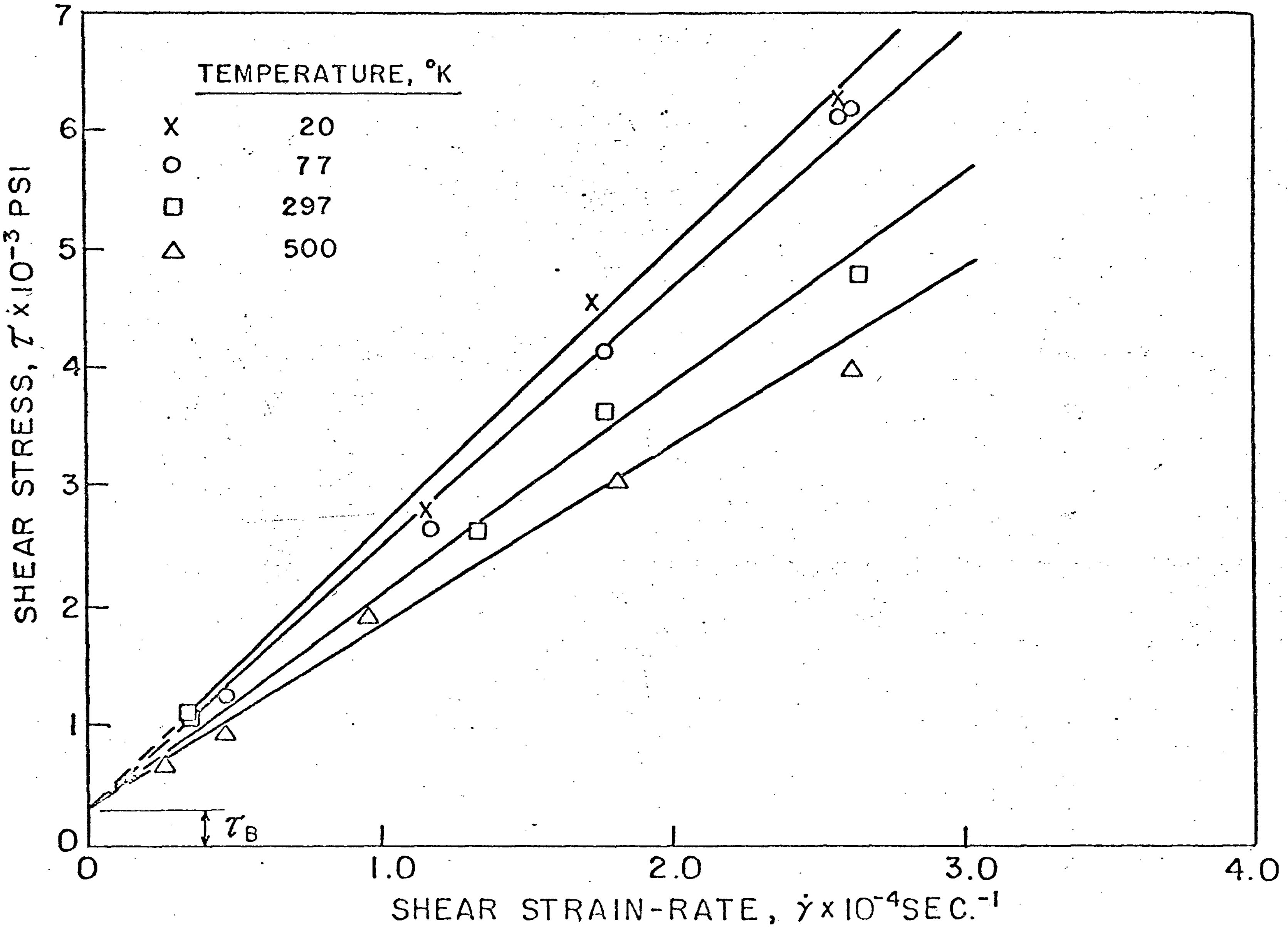

FIG. 3 SHEAR STRESS VERSUS SHEAR STRAIN-RATE FOR DYNAMIC SHEAR IN ALUMINUM SINGLE CRYSTALS.

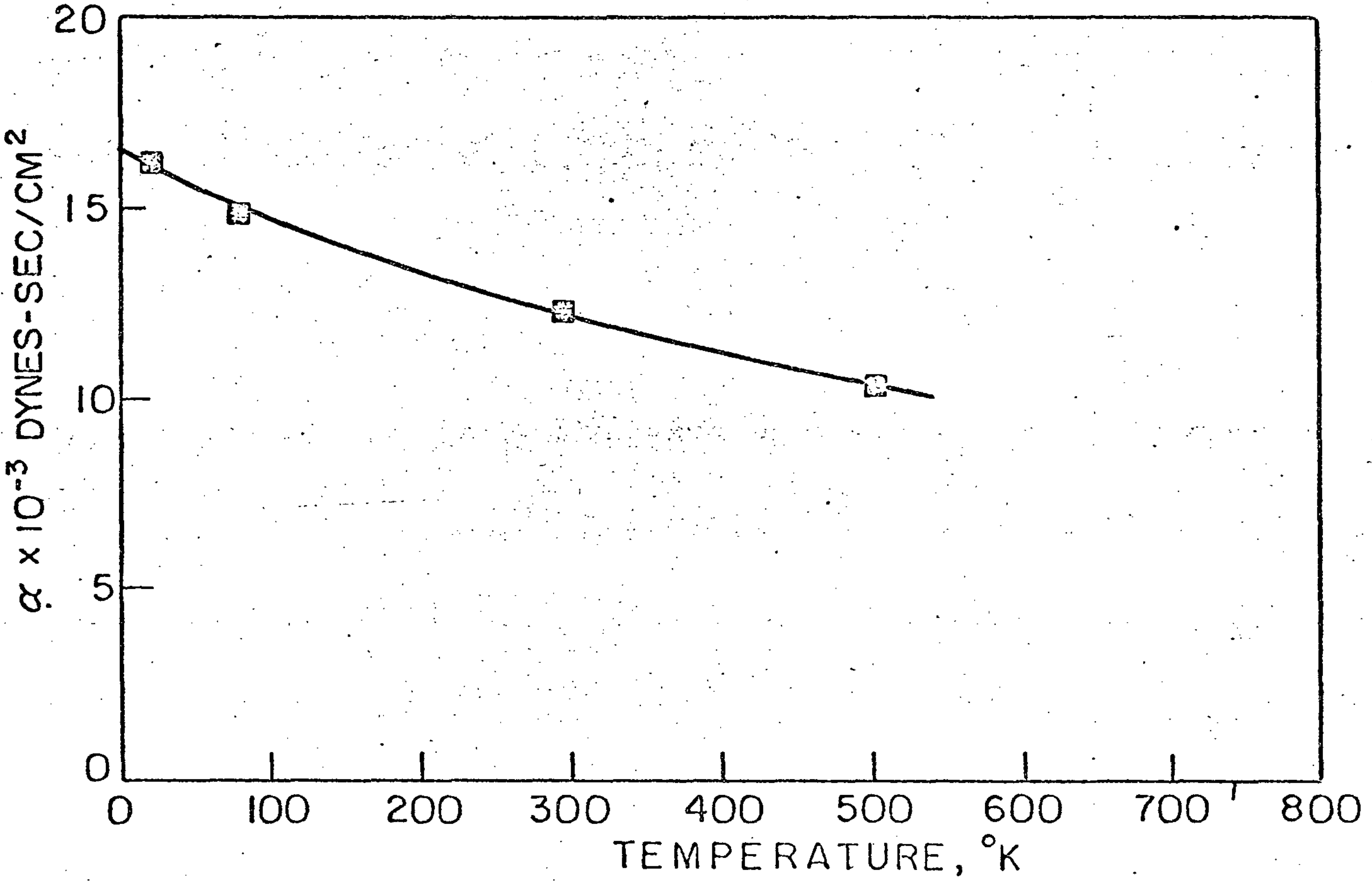

FIG. 4 THE SLOPE α OF THE SHEAR STRESS - SHEAR STRAIN-RATE CURVES VERSUS TEMPERATURE.

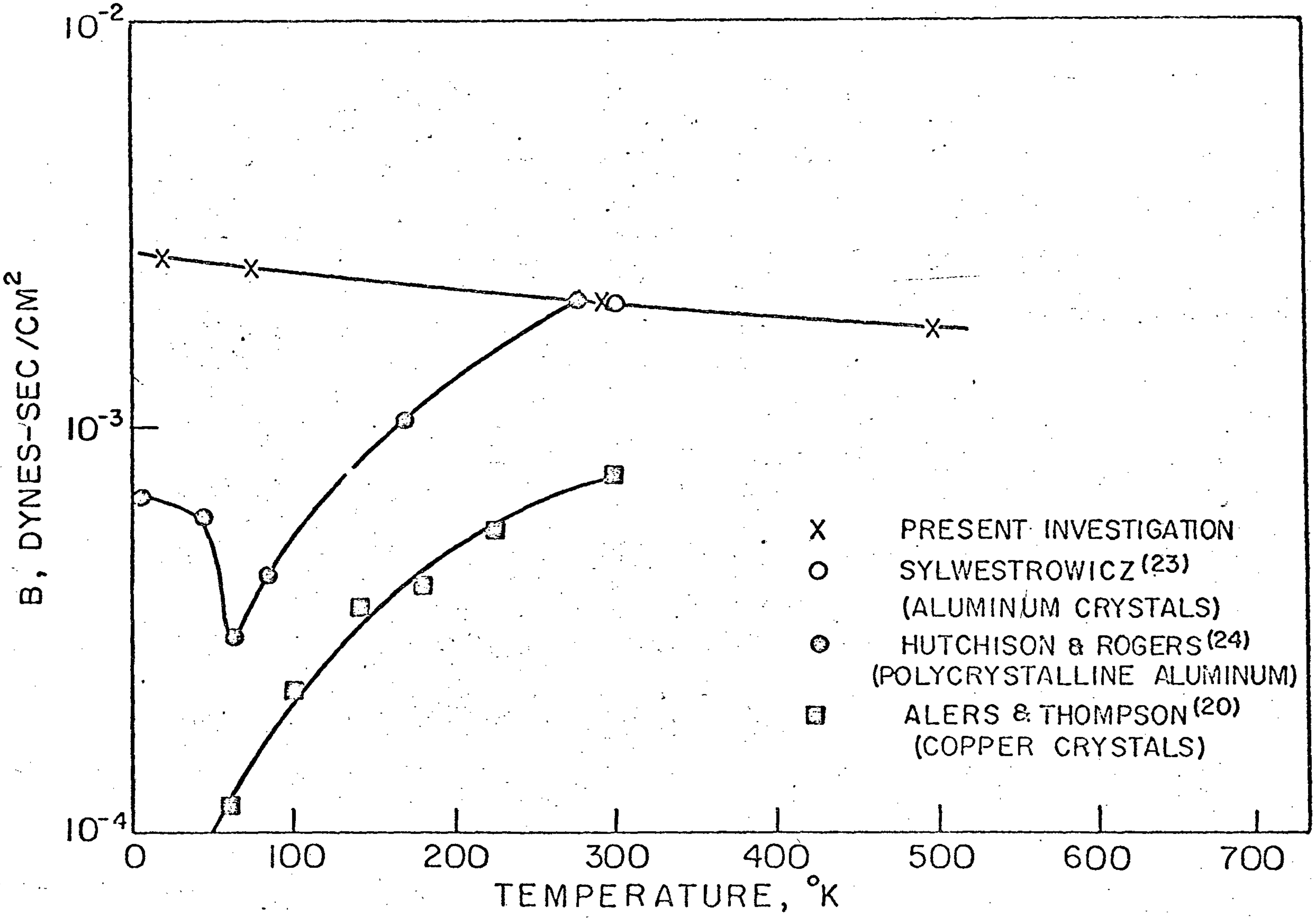

FIG. 5 EXPERIMENTAL DAMPING CONSTANTS FOR ALUMINUM AND COPPER VERSUS TEMPERATURE.

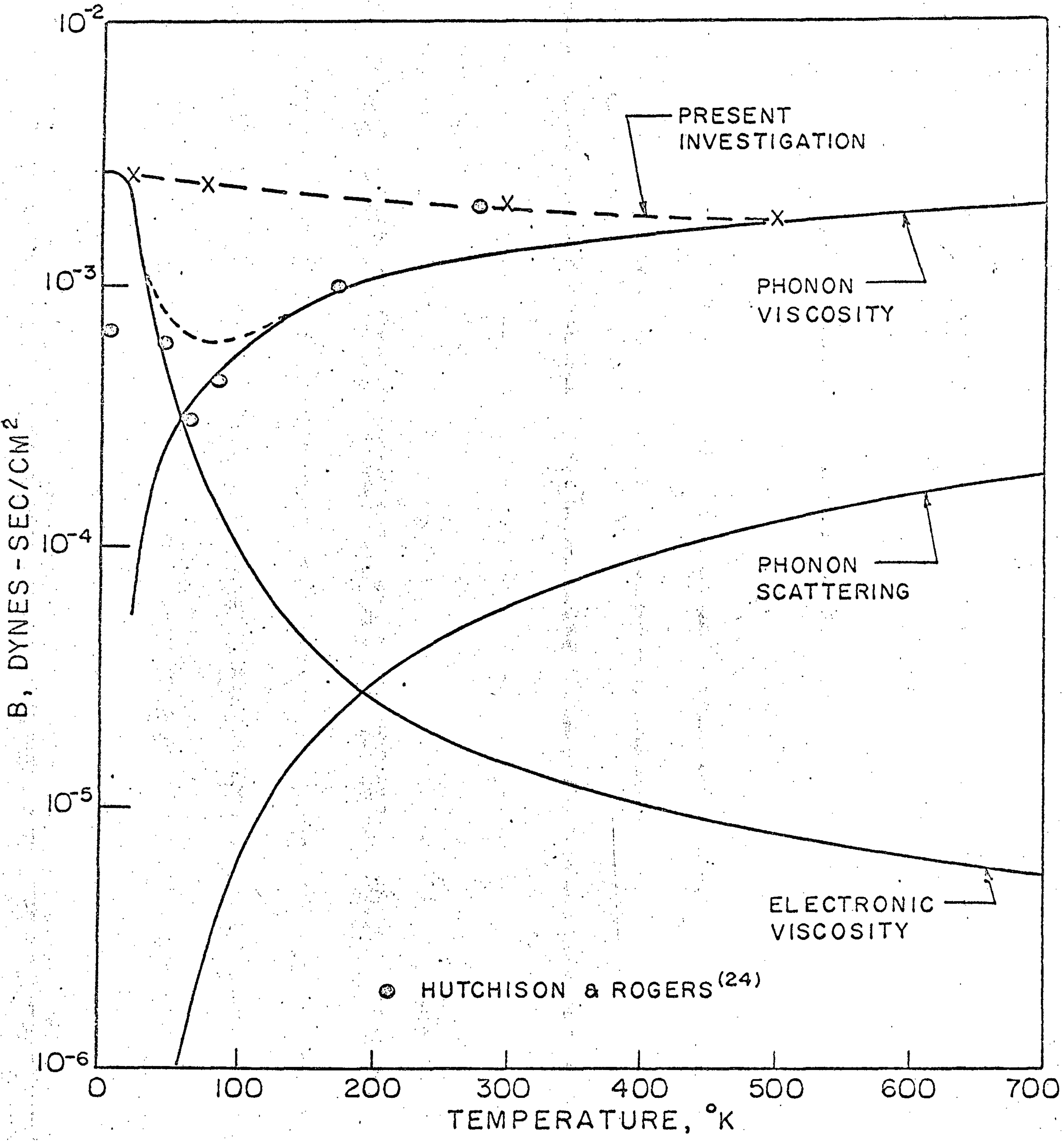

FIG. 6 THEORETICAL DAMPING CONSTANTS FOR PHONON SCATTERING, PHONON VISCOSITY AND ELECTRONIC VISCOSITY IN ALUMINUM.